Highlighting research from the Carbohydrate-based Bioactive Molecules and Supramolecular Materials Laboratory from the group of Dr Velasco-Torrijos (Maynooth University).

Glycosyl squaramides, a new class of supramolecular gelators

Amphiphilic glycosyl squaramides formed thermoreversible gels in polar organic solvents and hydroethanolic mixtures with high efficiency. Rheological analysis showed that these gels are robust and suitable for biomedical applications. These are the first reported examples of carbohydrate-squaramide conjugates capable of forming supramolecular gels.

As featured in:

See Ramon Moreira, Trinidad Velasco-Torrijos *et al.*, *Soft Matter*, 2020, **16**, 7916.

Check for updates

Glycosyl squaramides, a new class of supramolecular gelators†

Jessica Ramos,[a] Santiago Arufe,[b] Harlei Martin, [ID][a] Denise Rooney, [ID][ac]
Robert B. P. Elmes, [ID][ac] Andrea Erxleben, [ID][d] Ramon Moreira*[b] and
Trinidad Velasco-Torrijos [ID]*[ac]

Glycosyl squaramides were synthesised and evaluated as low molecular weight gelators. Amphiphilic glycosyl squaramides **5** and **6**, with a C-16 aliphatic chain, formed thermoreversible gels in polar organic solvents and 1:1 ethanol/water mixtures with high efficiency. Rheological analysis showed these gels achieve their structural stability 120 h after gelation and were robust, making them particularly suitable for biomedical applications. The interactions between solvent and gelator strongly influence SAFiN (Self-Assembled Fibrillar Network) formation, critical gelation concentration (CGC) and subsequent gel structure, as evidenced by SEM imaging of xerogels. Spectroscopic studies indicate that H-bonding is involved in the self-assembly of the glycosyl squaramides in organic solvents, while hydrophobic interactions are the major driving force for gel formation in the presence of water. The compounds described herein are the first reported examples of carbohydrate-squaramide conjugates capable of forming supramolecular gels.

Introduction

The design and formulation of low molecular weight gelators (LMWG) that are robust, malleable and with appropriate rheological properties is a key step to achieve state-of-the-art functional materials; these systems are highly sought after for their applications in nanoelectronics, tissue engineering and medical devices.[1,2] Numerous molecular building blocks have been investigated and reported to self-assemble, forming supramolecular gels; of these, materials with biological relevance and from sustainable sources, such as carbohydrates, have attracted much interest.[3,4] Typically the polar carbohydrates are combined with hydrophobic moieties (aliphatic and/or aromatic) that provide structural frameworks for self-assembling through non-covalent interactions. Squaramides have been studied extensively in supramolecular chemistry: due to their aromaticity and ability to act as effective hydrogen bond donors and acceptors, they have been used in the design of ion receptors[5,6] and lately, as organocatalysts.[7] Surprisingly, squaramide derivatives have begun to be investigated as supramolecular gelators only in recent years:

considering the structural characteristics of the few squaramide gelators reported so far, the presence of long hydrocarbon chains (C_{12} up to C_{18}) appeared to produce the gelation in organic solvents of a range of different polarities;[8,9] asymmetric squaramides with aryl sulphonamide substituents showed a marked propensity to induce gelation of alcohols,[10] while amphiphilic squaramides with polar tetraethylene glycol[11] or acidic functionalities[12,13] achieved hydrogelation. Carbohydrates are versatile, readily available molecules that occupy a prominent role in the preparation of biomimetic self-assembled materials[14,15] and LMWG with environmental applications.[16,17] Given the relevance of carbohydrates in many biological events and their applications in biomedical science,[18] in this work we explore the structural features required to modulate gelation capabilities of squaramides by combining them with galactosyl moieties, triazoles and aliphatic chains, and report the first example of glycosyl squaramides as highly efficient supramolecular gelators.

Experimental

Synthesis

General methods. All reagents for synthesis were bought commercially and used without further purification. Reactions were monitored with thin layer chromatography (TLC) on Merck Silica Gel F_{254} plates. Detection was effected by UV (λ = 254 nm) or charring in a mixture of 5% sulfuric acid-ethanol. Nuclear Magnetic Resonance (NMR) spectra were recorded using Bruker Ascend 500 spectrometer at 293 K. All chemical shifts

[a] *Department of Chemistry, Maynooth University, Maynooth, Co., Kildare, Ireland.*
E-mail: trinidad.velascotorrijos@mu.ie
[b] *Department of Chemical Engineering, Universidade de Santiago de Compostela,*
Rua Lope Gomez de Marzoa s/n, ES-15782, Santiago de Compostela, Spain
[c] *The Kathleen Lonsdale Institute for Human Health Research, Maynooth University,*
Maynooth, Co., Kildare, Ireland
[d] *School of Chemistry, National University of Ireland, Galway, Ireland*
† Electronic supplementary information (ESI) available. See DOI: 10.1039/d0sm01075h

were referenced relative to the relevant deuterated solvent residual peaks. Assignments of the NMR spectra were deduced using ^{1}H NMR and ^{13}C NMR, along with 2D experiments (COSY, HSQC and HMBC). Chemical shifts are reported in ppm. Flash chromatography was performed with Merck Silica Gel 60. Microwave (μW) reactions were carried out using a CEM Discover Microwave Synthesizer. Optical rotations were obtained from an AA-100 polarimeter and $[\alpha]_D$ values are given in 10^{-1} cm^2 g^{-1}. High resolution mass spectrometry (HRMS) was performed on an Agilent-LC 1200 Series coupled to a 6210 Agilent Time-Of-Flight (TOF) mass spectrometer equipped with an electrospray source in both positive and negative (ESI +/−) modes. Scanning Electron Microscope (SEM) images were taken on a HITACHI S-3200N Scanning Electron Microscope. Rheological measurements were performed on a stress-controlled Anton Paar Physica MCR301 rheometer using PP15/Al and a P-PTD 200/TG+H-PTD200. Differential Scanning Calorimetry (DSC) analysis was carried out on a PerkinElmer Pyris 6 instrument. The stainless steel crucibles for DSC (pan: Φ 6.7 × 2.6 mm & lid: Φ 7 × 2 mm), temperature range: −50 to 280 °C were supplied for Shanghai DiBo Laboratory Equipment Co., Ltd. FT-IR spectra were recorded on a PerkinElmer Spectrum 100 spectrophotometer, via ATR as a solid on a zinc selenide crystal or as a film on NaCl plates in the region 4000–400 cm^{-1}. Spectroscopic data for all compounds are provided in the ESI.†

3,4-Di(prop-2-yn-1-ylamino)cyclobut-3-ene-1,2-dione 1. Ethyl square (0.2 mL, 1.35 mmol), propargylamine (0.18 mL, 2.8 mmol) and triethylamine (0.75 mL, 5.4 mmol) were allowed to stir in ethanol (2 mL) for 16 h at room temperature. A precipitate formed, which was filtered using a sintered glass funnel, washed with ethanol and allowed to dry to give the pure product **1** (254 mg, 98%, pale yellow solid). ^{1}H NMR (500 MHz, DMSO-d_6) δ 7.79 (s, 2H, NH), 4.34 (d, J = 3.8 Hz, 4H, CH_2CCH), 3.36 (t, J = 2.5 Hz, 2H, CH$_2$CCH). ^{13}C NMR (125 MHz, DMSO-d_6) δ 183.2 (CO), 167.8 (C=C), 81.0 (CH$_2$$C$CH), 75.7 (CH$_2CCH$), 33.2 ($CH_2$CCH). IR (ATR): 3280, 3149, 2922, 1801, 1648, 1551, 1472, 1415, 1343, 1298, 1272, 1132, 972, 915, 827, 747, 670 cm^{-1}. HRMS (ESI+): m/z calculated for C$_{10}$H$_8$N$_2$O$_2$ + Na$^+$ [M + Na$^+$]: 211.0483, found 211.0479.

3,4-Di(2,3,4,6-tetra-O-acetyl-β-D-galactopyranosyl-1,2,3-triazol-4-ylmethylamino)cyclobut-3-ene-1,2-dione 2. Copper sulphate pentahydrate (20 mg) and sodium ascorbate (40 mg) were added to a solution of 2,3,4,6-tetra-O-acetyl-1-β-azido-D-galactopyranoside[19] (375 mg, 1.004 mmol) and **1** (90 mg, 0.478 mmol) in acetonitrile/water (4 mL/2 mL). The reaction was allowed to stir in the microwave at 100 °C until deemed complete by TLC analysis (10 min). The solvent was removed in vacuo. The residue was dissolved in dichloromethane (30 mL), washed with water (3 × 20 mL), and dried (MgSO$_4$). The mixture was filtered and the solvent was removed in vacuo to yield the crude product, which was purified by silica gel column chromatography (DCM : MeOH 98 : 2–93 : 7) to give the pure product **2** (362 mg, 81%, off-white solid). R_f = 0.5 (DCM : MeOH 9 : 1). $[\alpha]_D^{27}$ −8.0 (c 1, DCM). ^{1}H NMR (500 MHz, DMSO-d_6) δ 8.27 (s, 2H, triaz-H), 7.84 (s, 2H, NHCH$_2$-triaz), 6.25 (d, J = 9.3 Hz, 2H, H-1), 5.59 (t, J = 9.6 Hz, 2H, H-2), 5.46–5.40 (m, 2H, H-3 and H-4), 4.80 (d, J = 5.1 Hz, 4H, CH_2-triaz), 4.59–4.54

(m, 2H, H-5), 4.07 (ddd, J = 18.9, 11.6, 6.2 Hz, 2H, H-6 and H-6′), 2.18 (s, 6H, OAc), 1.99 (s, 6H, OAc), 1.94 (s, 6H, OAc), 1.80 (s, 6H, OAc). ^{13}C NMR (125 MHz, DMSO-d_6) δ 183.3, 170.41, 170.4, 169.9 (each CO), 169.0 (CO of OAc and C=C), 145.1 (C-triaz), 123.0 (CH-triaz), 84.7 (C-1), 73.4 (C-5), 70.9 (C-3/4), 68.2 (C-2), 67.8 (C-3/4), 62.0 (C-6), 38.9 (CH$_2$-triaz), 21.0, 20.9, 20.8, 20.4 (each CH$_3$ of OAc). IR (film on NaCl): 3155, 2938, 2121, 1754, 1653, 1581, 1431, 1371, 1220, 1052, 923, 598 cm^{-1}. HRMS (ESI+): m/z calculated for C$_{38}$H$_{46}$N$_8$O$_{20}$ + Na$^+$ [M + Na$^+$]: 957.2726, found 957.2741.

3,4-Di(β-D-galactopyranosyl-1,2,3-triazol-4-ylmethylamino)-cyclobut-3-ene-1,2-dione 3. **2** (167 mg, 0.18 mmol) was dissolved in methanol/water (4 mL, 2 mL). Triethylamine (0.1 mL) was added, and the reaction mixture was allowed to stir at 45 °C for 6 h. The solution was cooled, Amberlite H$^+$ was added and the mixture was allowed to stir for 30 min. The solution was filtered, and the solvent was removed in vacuo. Excess triethylamine was removed using the Schlenk line. The product was freeze-dried overnight to yield the pure product **3** (82 mg, 77%, white solid). $[\alpha]_D^{22}$ +3.0 (c 1, DMSO). ^{1}H NMR (500 MHz, DMSO-d_6) δ 8.24 (s, 2H, triaz-H), 7.88 (bs, 2H, NHCH$_2$-triaz), 5.54 (d, J = 9.2 Hz, 2H, H-1), 5.28 (d, J = 6.0 Hz, 2H, OH), 5.05 (d, J = 5.7 Hz, 2H, OH), 4.87 (s, 4H, CH_2-triaz), 4.74 (t, J = 5.7 Hz, 2H, OH), 4.69 (d, J = 5.6 Hz, 2H, OH), 4.07 (td, J = 9.3, 6.3 Hz, 2H, H-2), 3.83–3.79 (m, 2H, H-4), 3.76 (t, J = 6.1 Hz, 2H, H-5), 3.63–3.49 (m, 6H, H-3, H-6 and H-6′). ^{13}C NMR (125 MHz, DMSO-d_6) δ 183.2 (CO), 167.9 (C=C), 144.8 (C-triaz), 122.3 (CH-triaz), 88.6 (C-1), 78.9 (C-5), 74.2 (C-3), 69.8 (C-2), 68.9 (C-4), 60.9 (C-6), 39.1 (CH$_2$-triaz). IR (ATR): 3370, 2940, 2502, 1794, 1652, 1551, 1432, 1368, 1287, 1095, 1053, 1024, 892, 700 cm^{-1}. HRMS (ESI+): m/z calculated for C$_{22}$H$_{30}$N$_8$O$_{12}$ + Na$^+$ [M + Na$^+$]: 621.1881, found 621.1896.

N^4-[2-O-(2,3,4,6-Tetra-O-acetyl-β-D-galactopyranosyl)-ethyl]-N^2-3-4-dioxocyclobut-1-en-1-yl-hexadecylamino 5. 2-Aminoethyl 2,3,4,6-tetra-O-acetyl-β-D-galactopyranoside[20] (463 mg, 1.18 mmol) was dissolved in ethanol (10 mL) and added to a stirring solution of 3-ethoxy-4-hexadecylamino-3-cyclobutene-1,2-dione **4**[21] (216 mg, 0.59 mmol) in ethanol (10 mL). The reaction mixture was heated until it became a solution and then trimethylamine (0.5 mL, 3.55 mmol) was added. The mixture was stirred overnight at room temperature (rt). The solvent was removed under reduced pressure. The residue was purified by column chromatography (DCM : MeOH; 95 : 5) to give product **5** (388 mg, 92%, white solid); R_f = 0.77 (DCM : MeOH; 95 : 5); $[\alpha]_D^{22}$ = −6.6 (c 1.0 DCM). ^{1}H NMR (500 MHz, CDCl$_3$): 7.29 (s, 2H, CH$_2$CH$_2$NH and NHCH$_2$), 5.38 (d, J = 2.8 Hz, 1H, H-4), 5.17–5.12 (m, 1H, H-2), 5.01 (dd, J = 10.5, 3.4 Hz, 1H, H-3), 4.56 (d, J = 7.9 Hz, 1H, H-1), 4.18–4.09 (m, 2H, overlap of H-6, H-6′), 4.01–3.99 (m, 1H, OCH$_2$CH$_2$NH), 3.95–3.92 (m, 1H, H-5), 3.87–3.76 (m, 3H, OCH$_2$CH$_2$NH), 3.66–3.62 (m, 2H, NH CH$_2$), 2.13, 2.03, 2.00, 1.95 (each s, 3H, OAc), 1.64–1.58 (m, 2H, NHCH$_2$CH$_2$), 1.37–1.23 (m, 26H, NHC$_2$H$_4$(CH$_2$)$_{13}$CH$_3$), 0.85 (t, J = 6.9 Hz, 3H, CH$_3$). ^{13}C NMR (125 MHz, CDCl$_3$): δ 182.8, 182.4, 170.5, 170.4, 170.1, 169.9 (each CO), 168.1, 167.8 (each C=C), 101.4 (C-1), 70.9, 70.8 (C-5, C-3), 69.2 (C-2), 68.9 (OCH$_2$CH$_2$NH) 67.0 (C-4), 61.3 (C-6), 44.7 (OCH$_2$CH$_2$NH), 43.8 (NHCH$_2$C$_{15}$H$_{31}$), 31.9, 31.3, 31.2, 29.7,

29.6, 29.5, 29.4, 29.3, 29.2, 26.6, 26.3, 23.2, 22.7 (NHC$_2$H$_4$(CH$_2$)$_{13}$CH$_3$), 20.8, 20.7, 20.6, 20.5 (each CH$_3$ of OAc), 14.1 (NHC$_{15}$H$_{30}$CH$_3$). IR (DCM film on NaCl disk): 3173, 2956, 2917, 2850, 2117, 1801, 1751, 1649, 1578, 1470, 1437, 1371, 1227, 1175, 1133, 1059, 957, 907, 737 cm^{-1}. HRMS (ESI+): m/z calculated for C$_{36}$H$_{58}$N$_2$O$_{12}$ [M + H$^+$]: 711.4063, found 711.4083.

N^4-[2-O-(β-D-Galactopyranosyl)-ethyl]-N^2-3-4-dioxocyclobut-1-en-1-yl-hexadecylamino 6. Triethylamine (0.3 mL, 2 mmol) was added to a stirring solution of N^4-[2-O-(2,3,4,6-tetra-O-acetyl-β-D-galactopyranosyl)-ethyl]-N^2-3-4-dioxocyclobut-1-en-1-yl-hexadecyl-amino 5 (335 mg, 0.39 mmol) dissolved in dichloromethane/methanol/water (3 mL, 6 mL, 3 mL). The mixture was stirred for 18 h at 40 °C. The reaction mixture was concentrated under reduced pressure to afford product 6 (288 mg, 98%, white solid); $[\alpha]_D^{22}$ = −0.8 (c 1.0 EtOH). ^{1}H NMR (500 MHz, DMSO-d_6): 7.50 (s, 2H, overlap of CH$_2$CH$_2$NH and NHCH$_2$), 4.82 (d, J = 4.1 Hz, 1H, OH), 4.74 (d, J = 5.0 Hz, 1H, OH), 4.68–4.64 (m, 1H, OH), 4.39 (d, J = 4.3 Hz, 1H, OH), 4.13 (d, J = 7.4 Hz, 1H, H-1), 3.84–3.79 (m, 1H, OCH$_2$CH$_2$NH), 3.73–3.62 (m, 4H, overlap of OCH$_2$CH$_2$NH and H-5), 3.54–3.44 (m, 4H, overlap of NHCH$_2$, H-6 and H-6′), 3.40–3.25 (m, overlap of H-2, H-3 and H-4), 1.51–1.48 (m, 2H, NHCH$_2$CH$_2$), 1.26–1.23 (m, 26H, NHC$_2$H$_4$-(CH$_2$)$_{13}$CH$_3$), 0.85 (t, J = 7.1 Hz, 3H, CH$_3$). ^{13}C NMR (125 MHz, DMSO-d_6): δ 182.9, 182.8 (each CO), 172.4, 168.0 (each C=C), 104.4 (C-1), 75.8, 73.8, 70.9 (C-4, C-3, C-2), 69.4 (OCH$_2$CH$_2$NH) 68.6 (C-5), 60.9 (C-6), 44.1 (OCH$_2$CH$_2$NH), 43.7 (NHCH$_2$C$_{15}$H$_{31}$), 31.7, 31.3, 31.2, 29.7, 29.6, 29.5, 29.4, 29.3, 29.2, 29.1, 26.6, 26.3, 22.6 (NHC$_2$H$_4$(CH$_2$)$_{13}$CH$_3$), 14.4 (NHC$_{15}$H$_{30}$CH$_3$). IR (KBr disk): 3449, 3232, 2918, 2851, 1797, 1641, 1571, 1470, 1425, 1350, 1171, 1078, 900, 780, 719, 604 cm^{-1}. HRMS (ESI+): m/z calculated for C$_{28}$H$_{50}$N$_2$O$_8$ [M + H$^+$]: 543.3567, found 543.3646.

Preparation of the gels

A given amount of the gelators 2, 3, 5 and 6 were mixed with 1 mL of the required solvent in a glass vial with a lid. The mixture was heated slowly until completely dissolved (or soni-cated for 1 min until completely dissolved). Then the solution was allowed to cool to room temperature (rt). After 2 h, gelation was checked visually by inversion of the vial. Gel formation was considered to take place if no flow was observed upon vial inversion. Further analysis on the gels was conducted 120 h after formulation.

Determination of critical gel concentration (CGC). The minimal gel concentration required for the gelator to entrap the required solvent (CGC) was determined as follows: to a solution of gelator (20 mg) in a given solvent (1 mL), 0.2 mL aliquots of the solvent were added. For each aliquot the sample was heated and/or sonicated, then allowed to cool to rt. The gelation was then evaluated by the inverted test tube method to ascertain if the solvent was flowing freely. This process was repeated until partial gelation occurred or until the inverted test tube method showed free flowing solvent.

Determination of the gel to sol transition temperature (T_{gs}). T_{gs} were determined by heating the gel sample on a water bath and monitoring the temperature of the melting process.

Rheological analysis

Rheological characterisation was carried out using a controlled stress rheometer (MCR 301, Anton Paar, Austria) with parallel plates (15 mm diameter, 0.5 mm gap) at selected temperature of 10 °C under the T_{gs} (±0.1 °C). Gels to be tested were placed between the plates and the excess volume of sample was trimmed and the edge was coated with paraffin to prevent solvent evaporation during the measurement. A rest time of 15 min was applied to all samples prior to any measurements. Small Amplitude Oscillatory Shear (SAOS) tests were performed. The linear viscoelastic region (LVER) was determined by means of a strain sweep (γ, 0.01–100%) at a frequency of 1 Hz. The mechanical spectra of gels were obtained by frequency sweep test from 0.1 to 100 rad s^{-1} of angular frequency at 0.1% strain (inside the LVER of the samples) to determine the storage, G' (Pa) and loss, G'' (Pa) modulus and the loss tangent (tan δ = G''/G').

Differential scanning calorimetry (DSC) analysis

The thermal reversibility of the gels was investigated by DSC under a nitrogen atmosphere. DSC thermograms were recorded for heating/cooling cycles. The temperature ranges for the experiments were decided at selected temperature of 10 °C under the T_{gs} and the boiling point of the solvent. Temperature cycles were set at a constant rate of 2 °C min^{-1}. Stainless steel pans of medium pressure were used for the gels tested. A small quantity of the gel (20–40 mg) made at the CGC in a closed vial was transferred with a spatula to the pan which was closed under pressure. A reference pan was filled with the gelation solvent alone.

SEM imaging

A small quantity of the gel made at the CGC with the required solvent in a closed vial was transferred with a spatula to the metal stub (previously prepared with a double-sided adhesive tape with a conductive carbon tab). The xerogel was formed on the stub by allowing evaporation of the solvent (with freeze drying when sample contained water). If required, the samples were sputter-coated with a layer of gold.

FTIR spectroscopic analysis

FT-IR spectra were recorded at increasing time intervals, from 0 min (immediately after dissolving gelator at CGC in the required solvent) recording every 5 min until X-end min as specified in each experiment. Measurements were carried out in a closed cell or in a universal attenuated total reflection (ATR) accessory (diamond crystal) for liquids. The sample was handled so as to prevent solvent evaporation during the gelation process.

Results and discussion

Synthesis

Early work by Hamachi and co-workers[22] screened the gelation abilities of several carbohydrate-amino acid conjugates, revealing that N-acetyl galactosamine and galactose were the more effective
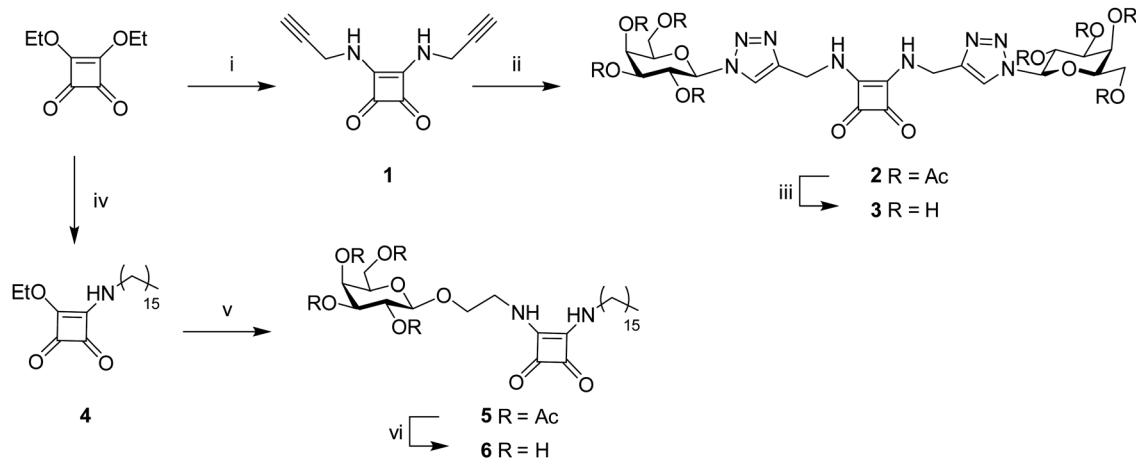
Scheme 1 *Reagents and conditions*: (i) $C_3H_3NH_2$, EtOH, N_2, 16 h, 98%; (ii) 2,3,4,6-tetra-*O*-acetyl-1-β-azido-D-galactopyranoside, $CuSO_4\cdot5H_2O$/Na Asc, CH_3CN/H_2O, 100 °C, μW, 10 min, 81%; (iii) MeOH, NEt_3, H_2O, 45 °C, 6 h, 77%; (iv) EtOH, $C_{16}H_{33}NH_2$, rt, 16 h, 49%; (v) EtOH, tetra-*O*-acetyl-1-β-*O*-2-aminoethyl-D-galactopyranoside, NEt_3, rt, 16 h, 92%; (vi) DCM/MeOH/H_2O (1:2:1), NEt_3, 40 °C, 18 h, 98%.
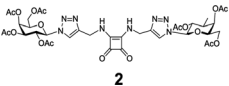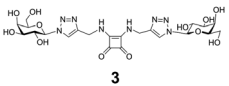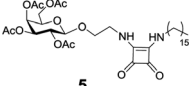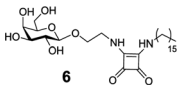
supramolecular gelators. For synthetic convenience, in the present study we focused on galactosyl derivatives (Scheme 1). Symmetric digalactosyl squaramides were prepared by reaction of diethyl squarate with propargylamine to give *N*,*N*-dipropargyl squaramide **1**. Microwave assisted CuAAC reaction with 2,3,4,6-tetra-*O*-acetyl-1-β-azido-D-galactopyranoside[19] produced compound **2**, in which the galactosyl moieties are connected to the squaramide with triazolyl groups. The acetyl protecting groups in the sugar were removed under mild basic conditions to afford compound **3**. Alternatively, diethyl squarate was reacted with hexadecylamine to install an aliphatic chain and give compound **4**,[21] which was then reacted with tetra-*O*-acetyl-1-β-*O*-2-aminoethyl-D-galactopyranoside[20] to produce galactosyl squaramide **5**. Hydrolysis of the acetyl esters in mild basic conditions gave amphiphilic compound **6**.

Gelation ability

The ability of the galactosyl-squaramides conjugates **2**, **3**, **5** and **6** to induce the formation of supramolecular gels was then screened in a range of solvents of different polarities and structural characteristics (Table 1). Gel formulation was investigated by sonication and thermal treatment (heating to 50 °C and cooling). Gel formation was observed after cooling down to rt in less than 2 h and in less than 5 min upon sonication, according to the "inverted test tube" method (Fig. 1).

Acetylated digalactosyl squaramide **2** was only able to form aggregates in ethyl acetate, which turned into an opaque gel upon further heating or sonication. Compound **2** also formed a weak gel in ethanol only upon sonication, which was found to be very unstable, breaking even upon gentle shaking. The deprotected

Table 1 Gelation abilities of squaramides **2**, **3**, **5** and **6** in different solvents: physical appearance, CGC (Critical Gelation Concentration, w/v%) and gel–sol transition temperature T_{gs} (°C) at the specified CGC

	2	3	5	6
Pentane	PS	I	I	I
Hexane	PS	I	I	I
Heptane	S	I	PS	PS
Pet. ether	I	I	I	I
Cyclohexane	I	I	PG	PG
Petrol	PS	I	PG	PS
Toluene	S	I	S	PS
Et_2O	I	I	I	PS
Chloroform	S	I	S	PS
DCM	S	I	S	I
EtOAc	A/OG(2)	I	OG(1.4)/T_{gs}(29–37)	PS
$DMSO:H_2O$ (1:1)	—	—	A	A
DMSO	—	—	S	S
MeCN	S	PS	OG(0.9)/T_{gs}(24–30)	PS
EtOH	TG*(2)	I	OG(1.7)/T_{gs}(26–29)	A
MeOH	I	PS	PG	PG
$EtOH:H_2O$ (1:1)	S	S	OG(0.7)/T_{gs}(50–57)	TG(0.1)/T_{gs}(48–60)
H_2O	PS	S	I	PS

S = soluble, PS = partial soluble, I = insoluble, A = aggregates, PG = partial gelation, TG = translucent gel, OG = opaque gel. * Gelation only occurred upon sonication.
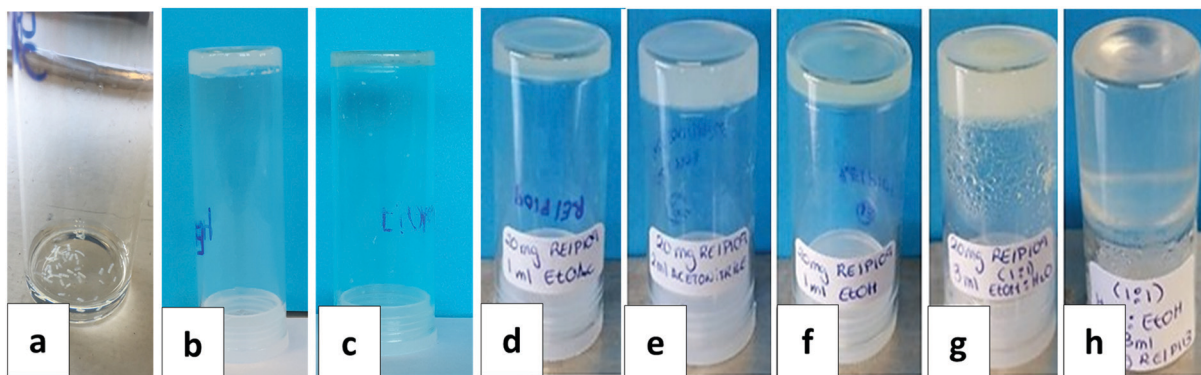
Fig. 1 Physical appearance of the squaramide-gels: (a) **2** aggregates in EtOAc; (b) **2** in EtOAc; (c) **2** in EtOH; (d) **5** in EtOAc; (e) **5** in MeCN; (f) **5** in EtOH; (g) **5** in EtOH : H$_2$O (1 : 1); (h) **6** in EtOH : H$_2$O (1 : 1).

digalactosyl derivative **3** failed to induce the gelation of any of the solvents tested. On the other hand, monogalactosyl squaramides **5**, featuring the C$_{16}$ aliphatic chain, was found to be a much more efficient gelator, forming gels in relatively high polarity solvents such as ethyl acetate, acetonitrile, ethanol and a 1 : 1 ethanol/water mixture, with CGC ranging from 0.7 (1 : 1 ethanol/water) to 1.7% (ethanol) w/v. Monogalactosyl squaramide **6**, which features free hydroxyl groups, was able to form a translucent gel exclusively in 1 : 1 ethanol/water mixture with 0.1% w/v CGC, which classified this compound as a "supergelator" (CGC < 1%).[23] These results indicate that triazolyl groups in **2** and **3** do not seem to confer sufficient hydrophobicity to produce efficient solvent gelation, unlike the hydrocarbon chain in **5** and **6**. The galactosyl groups (protected or deprotected) appear to modulate the solubility of the conjugates in each of the solvents and hence the CGC. Interestingly, the glycosquaramides **5** and **6** were efficient gelators of 1 : 1

ethanol/water, possibly due to the formation of three dimensional SAFiNs (Self-Assembled Fibrillar Networks) capable of entrapping large volumes of the solvent mixture. However, **6** was not capable of gelling either ethanol or water alone, resulting in aggregation or partial solubility, respectively.

Rheological evaluation

The viscoelastic properties of the gels formed by monogalactosyl squaramides **5** and **6** were investigated by SAOS (Fig. 2). Strain sweeps at 1 Hz were performed to evaluate the LVER and mechanical spectra (frequency sweeps) of the gels formed by **5** and **6** in different solvents. Mechanical spectra of the gels were recorded after 24, 96, 120 and 144 h to evaluate the rheological stability of their structure; G' (storage, or elastic modulus) and G'' (loss, or viscous modulus) values did not significantly change after 120 h. Therefore, the gels were studied at 10 °C and 120 h after formation. Concerning strain sweeps, gelator **5**
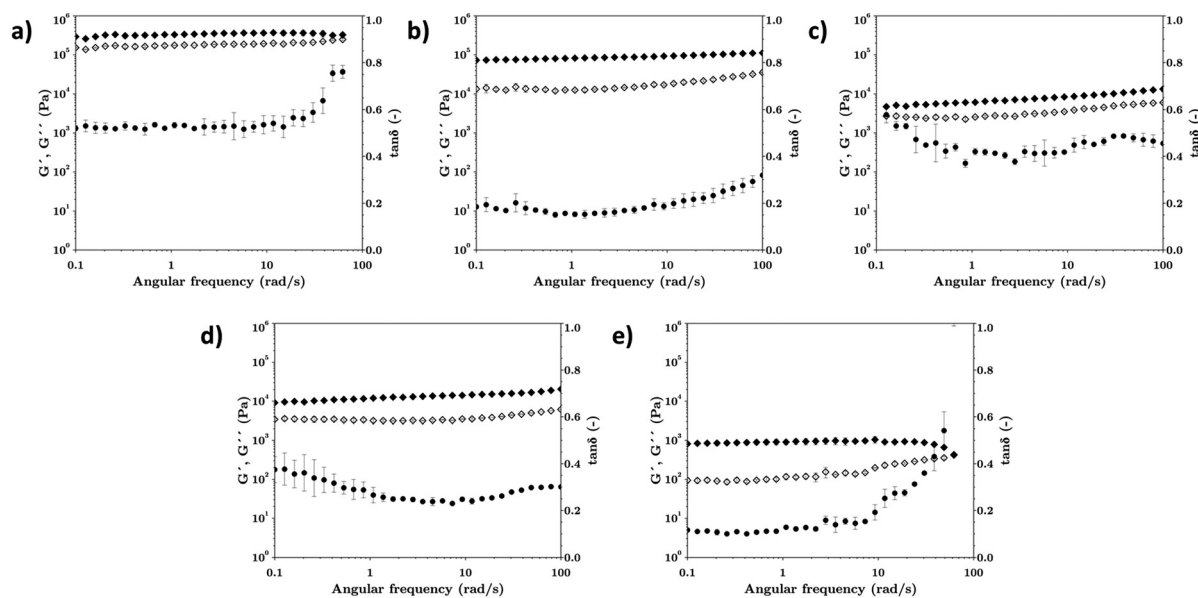

Fig. 2 (SAOS) Frequency sweep at a strain of 0.1% for gels formed by gelator **5** (a–d) and **6** (e) at 10 °C at a strain of 0.1% in: (a) EtOH (1.7% w/v) tan δ < 1; (b) EtOAc (1.4% w/v), tan δ < 0.5.; (c) MeCN (0.9% w/v), tan δ < 1; (d) EtOH : H$_2$O 1 : 1 (0.7% w/v), tan δ < 0.5; (e) EtOH : H$_2$O 1 : 1 (0.1% w/v), tan δ < 0.15. G' (♦); G'' (◊); tan δ (●).

Paper

Table 2 SAOS results for **5** (per-acetylated-monogalactosyl squaramide) and **6** (monogalactosyl squaramide) at 10 °C and after 120 h of gel formation. The data are displayed from the strongest (top) to the weakest (bottom) gel

Compound	Solvent	CGC (%w/v)	G' (Pa) at strain $< 0.1\%$	Strain (%) at ($G' = G''$)	G' (Pa)	$\tan\delta$
5	EtOH	1.7	$(4-3) \times 10^5$	0.5	$(2.9-3.3) \times 10^5$	0.51–0.89
	EtOAc	1.4	$(2-1) \times 10^5$	0.8	$(0.7-1.1) \times 10^5$	0.19–0.32
	MeCN	0.9	$(3-2) \times 10^4$	20	$(0.4-2.5) \times 10^4$	0.70–0.45
	EtOH : H_2O	0.7	$(3-1) \times 10^4$	70	$(1.0-2.1) \times 10^4$	0.34–0.30
6	EtOH : H_2O	0.1	$(2-1) \times 10^3$	10	$(0.9-1.0) \times 10^3$	0.12–0.13

shows the typical effect of gelator concentration independently of, in this case, the nature of the solvent during strain sweep tests. G' value reflects the structural strength of the gel and the cross point ($G' = G''$, Table 2) can be considered the beginning of the point at which the gel breaks and starts to flow.[24] Firstly, the G' at low strains (related to yield stress of the gel) varies from *ca.* 10^4 to 6×10^5 Pa when concentration varies from 0.7 w/w (**5** in 1 : 1 ethanol/water) and 0.9 w/w (**5** in acetonitrile) to 1.7 w/w (**5** in ethanol). Higher gelator concentration promotes chain interactions leading to a stronger network structure. Secondly, the cross point appears at low strains (0.5–0.8%) with high gelator concentration, meaning a more brittle structure. In fact, the gel formed by **5** in 1 : 1 ethanol/water is the softer gel obtained with gelator **5** and it maintains the solid character predominantly up to 70% of strain. Finally, the strain sweep corresponding to the gel formed by **6** in 1 : 1 ethanol/water shows the weakest characteristics ($G' = 10^3$ Pa, at low strain) due to the low gelator concentration (0.1 w/w). This gel has an intermediate cross point at 10% of strain, due to its different structural features in comparison to gelator **5**. A unique strain of 0.1% was selected for all samples to determine the mechanical spectra of all gels, since noisy results were obtained at lower strains. In the frequency sweeps, the high frequency region corresponds to short time behaviour and the low frequency zone mimics long-term behaviour. All gels showed $G' > G''$ throughout the angular frequency range that was studied, with low values of $\tan\delta$ (Table 2), indicating that the elastic nature of the samples prevailed over the viscous one. In general, low dependence of G' with angular frequency was found, while the G'' modulus, in some cases (Fig. 2a and d), increased at high frequencies, giving as a result a relevant increase of $\tan\delta$. This fact indicates that, for these samples, the rheological behaviour at short time is more influenced by the viscous response of the material. The gels formed by **5** in ethyl acetate and 1 : 1 ethanol/water had the lowest values of $\tan\delta$, showing that they have more solid character than those formed by **5** in either acetonitrile or ethanol (Fig. 2a–d). The strongest (and more concentrated system) gel was formed by **5** in ethanol, presenting the highest values of G' and G'' (Table 2). The gel formed by compound

6 in 1 : 1 ethanol/water mixture (Fig. 2e) showed the most relative elastic character reported in this study, with $\tan\delta$ values lower than 0.15 (Table 2). Remarkably, this gel maintained its structural integrity and rheological characteristics months after its original formulation (Fig. S1, ESI†). This property is particularly important for soft materials useful for biomedical applications.[25]

Thermal analysis

T_{gs} and DSC measurements. The thermoreversible behaviour of the gels formed in different solvents by compounds **5** and **6** was studied by measuring gel–sol transition temperatures (T_{gs}) and DSC analysis (Table 3 and Fig. 3), which was carried out 120 h after formulation to ensure that the gel formation was complete (according to rheological results). The thermograms in Fig. 3a–d show the endotherms (gel to sol transitions) and exotherms (sol to gel transitions) for the gels formed by gelator **5** in different solvents; the endotherms in the first heating cycle appear at temperatures that correlate well with the T_{gs} determined by the "melting" method for gels of **5** in organic solvents (Table 3, entries 1–3). The thermograms of the gels formed by **5** and **6** in 1 : 1 ethanol/water mixture showed less defined transitions than the gels formed from a single solvent. The occurrence of flat thermal events has been previously reported when polysaccharide hydrogels were treated with mixtures of water and ethanol in different ratios. The loss of definition was attributed to the interference of the alcohol with the gel network;[26] in the current work, it likely indicates that the gels were thermally stable under the conditions of the analysis and require longer time to show breaking/forming of intermolecular interactions. For all gels, it was observed that the third cycle, which was another heating cycle, showed lower T_{gs} values than the first cycle. This is consistent with rheological results, as the self-assembled fibrillar network that form the gels needs 120 h to reach completion.

Gel morphologies

The morphology of the xerogels formed by galactosyl-squaramide conjugates **5** and **6** was investigated using SEM imaging (Fig. 4). The density of the fibre network and the extent of fibre

Table 3 T_{gs} (°C) by heating and monitoring the meting temperature ("melting" method) and DSC transition temperatures (gel-to-sol and sol-to-gel) of thermoreversible squaramide-gels **5** and **6** for two heating (1st and 3rd cycles) and two cooling (2nd and 4th cycles) cycles at the specified CGC

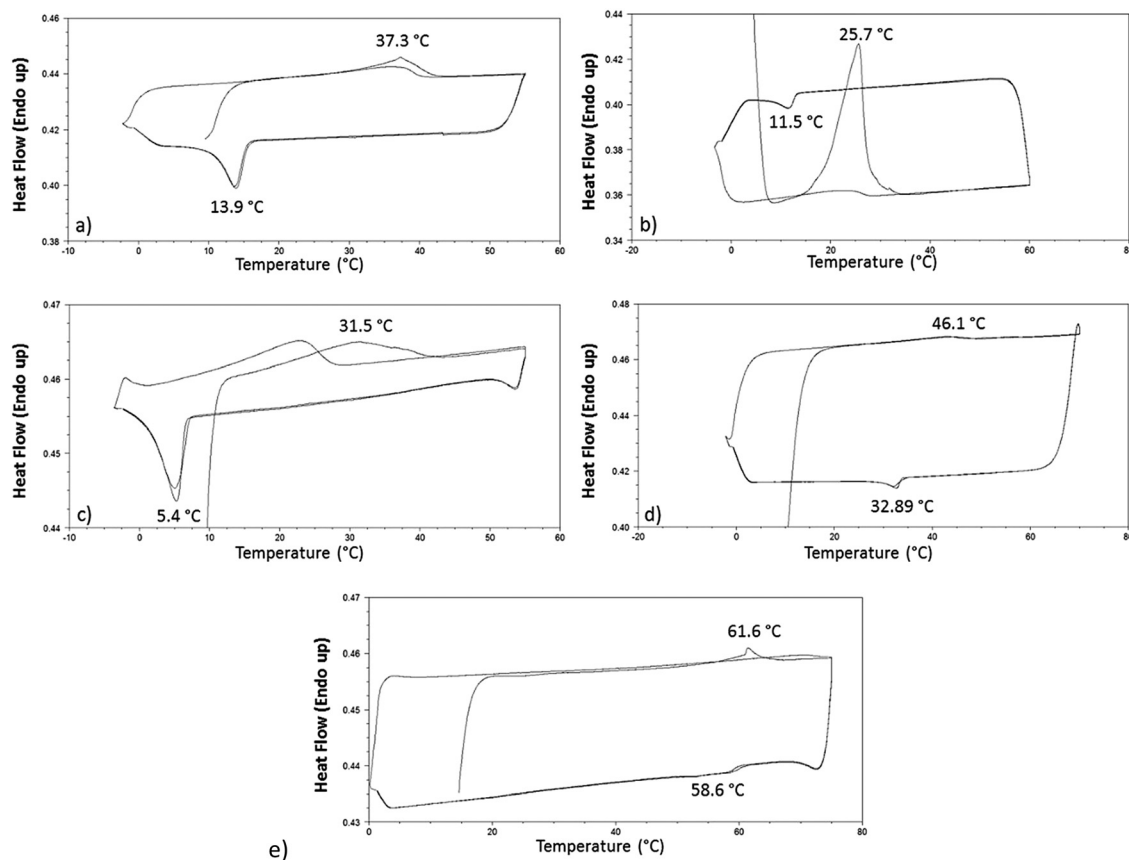| Entry	Gelator	Solvent	T_{gs} (°C)	1st cycle (heating) (°C)	2nd cycle (cooling) (°C)	3rd cycle (heating) (°C)	4th cycle (cooling) (°C)
1 (Fig. 3a)	5	EtOAc	29–37	37.3	13.9	36.7	13.8
2 (Fig. 3b)	5	MeCN	24–30	25.7	11.5	24.2	11.1
3 (Fig. 3c)	5	EtOH	26–29	31.5	5.4	23.3	5.0
4 (Fig. 3d)	5	EtOH : H_2O (1 : 1)	50–57	46.1	32.9	43.6	32.3
5 (Fig. 3e)	6	EtOH : H_2O (1 : 1)	48–60	61.6	58.6	53.4	57.9

Fig. 3   DSC of monogalactosyl-squaramide: (a) **5** in EtOAc (1.4% w/v); (b) **5** in MeCN (0.9% w/v); (c) **5** in EtOH (1.7% w/v), (d) **5** in EtOH : H$_2$O 1 : 1 (0.7% w/v) and (e) **6** in EtOH : H$_2$O 1 : 1 (0.1% w/v) during the two heating/two cooling cycles. The sample was heated from 0 °C to a temperature lower than the boiling point of the solvent used, at 2 °C min^{-1} and cooling the same range of temperature. Reproducible/duplicated cycles for each sample.
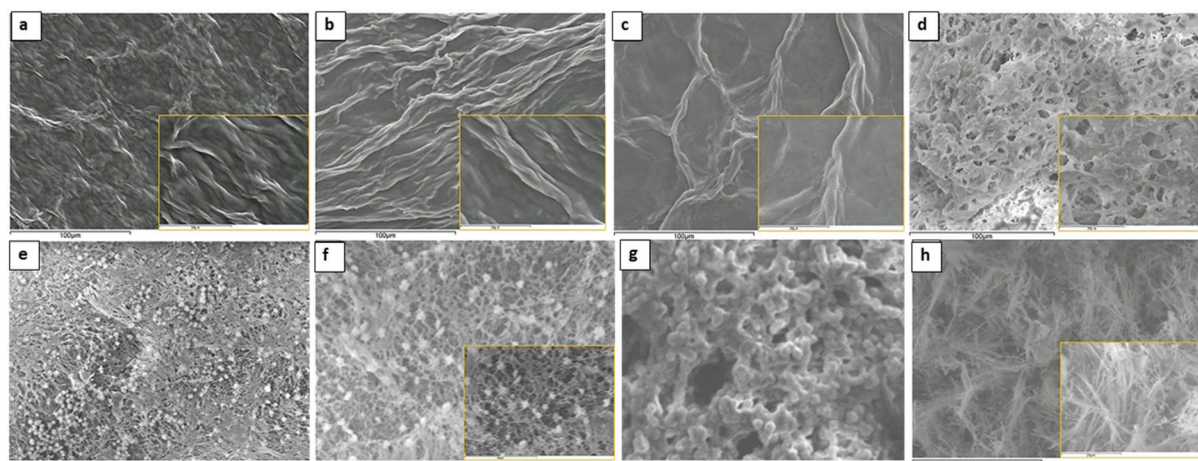

Fig. 4   SEM image of xerogels from gels formed by: (a) **5** in EtOAc; (b) **5** in MeCN; (c) **5** in EtOH; (d) **5** in EtOH : H$_2$O (1 : 1); (e and f) **6** in EtOH : H$_2$O (1 : 1); (g) **6** in EtOH; (h) **6** in DMSO : H$_2$O (1 : 1). Scale bar: (a–d), 100 μm; inset 50 μm; (e), 100 μm; (f), 80 μm; inset 50 μm; (g), 60 μm; (f), 60 μm; inset 50 μm. All gels were prepared at CGC.

cross-linking not only influences the mechanical properties of supramolecular gels, but also their morphological characteristics.[27] The appearance of the xerogels of the acetylated monogalactosyl squaramide **5** formed in ethyl acetate and acetonitrile (Fig. 4a and b) is similar, with packed fibrous-like structures that seem to be formed from folding of fine lamellar structures. This suggests a similar pattern in the self-assembly mode of **5** in these polar aprotic organic solvents, in which H-bonding interactions between squaramide groups can take place, with the carbohydrates exposed to the solvent and aliphatic chains forming lamellar like structures
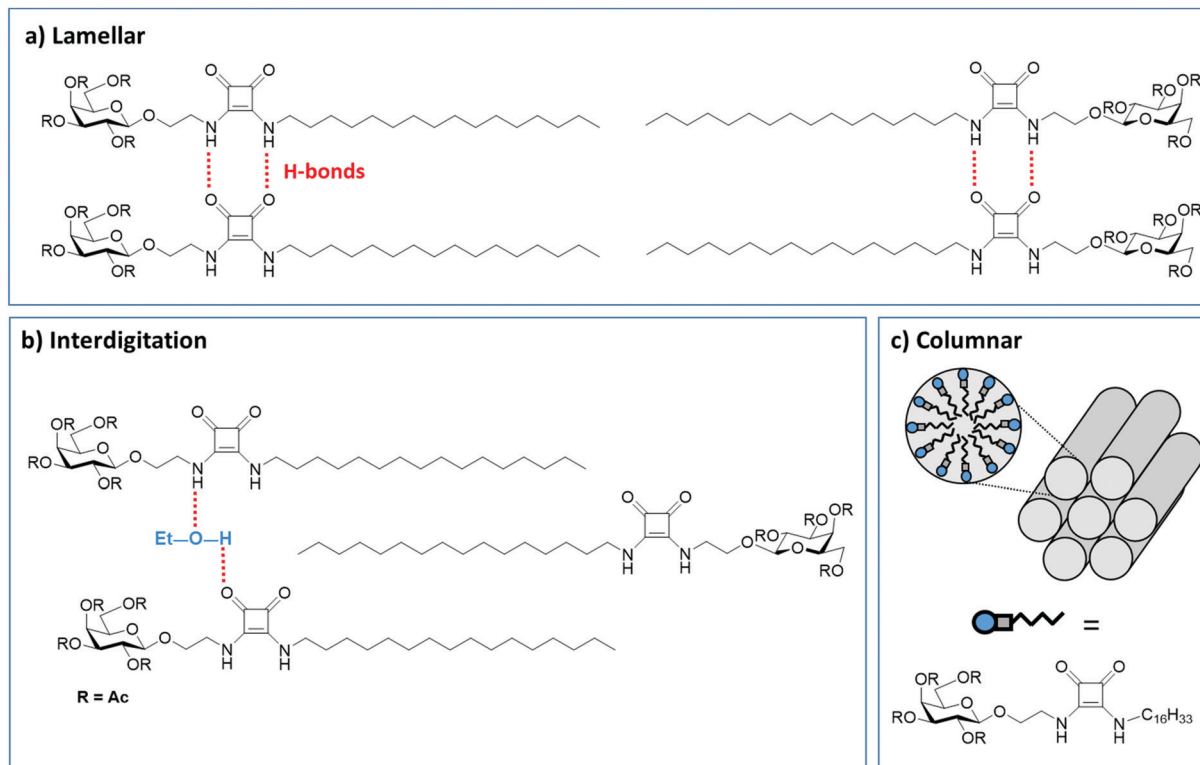
Fig. 5 Proposed self-assembly mode for glycosquaramide amphiphiles **5** and **6**: (a) lamellar-like in polar aprotic solvents; (b) ethanol-induced interdigitation; (c) water-induced columnar phases.

(possible arrangement shown in Fig. 5a). Although acetonitrile has both H-bond donor and acceptor character, it is a significantly weaker H-bond acceptor than ethyl acetate.[28] The higher concentration of **5** (1.4% w/v), required to form the gel in ethyl acetate results in a more densely packed structure (Fig. 4a). Interestingly, the xerogel image of **5** in ethanol shows a less densely packed structure, in which thicker fiber like structures are observed (Fig. 4c); ethanol has strong H-bond donor and acceptor character and may interfere in the H-bonding network of the squaramides and consequently, in the self-assembly pattern, *e.g.* solvation of ethanol of polar parts of the molecule can lead to interdigitation (Fig. 5b).[29] Ethanol solvation of gelator **5** can also account for the large CGC in this solvent (1.7% w/v), which in turn impacts on the rheological properties. XRPD of xerogels from **5** in single solvents showed a very similar broad pattern (Fig. S2a–c, ESI†). However, a more drastic change in the appearance of the xerogels formed by **5** was observed in ethanol:water 1:1 mixture, whereby SEM images showed a highly porous structure (Fig. 4d). Aromatic interactions between the squaramide rings[30] and hydrophobic contacts in the aliphatic chains can play a major role for self-assembly processes in the presence of water. For the xerogel of the deprotected galactosyl squaramide **6** in ethanol:water 1:1 mixture yet a different morphology of the xerogel can be appreciated, consisting in this case in a mat of entangled microfibers (Fig. 4e and f). Globular structures can be observed throughout the xerogel, which resemble the structure of porous aggregates formed by **6** in ethanol (Fig. 4g). This effect could be due to the slow dynamics of SAFiN formation as evidenced by the rheological study, which could lead

to competing self-assembly processes taking place in the solvent matrix. In contrast, only fibrils are observed in the xerogel of aggregates formed by **6** in DMSO:water 1:1 mixture (Fig. 4h). The presence of water can lead to phase transitions from lamellar to columnar type structures, as a result of the hydration of the polar groups on the glycosquaramide amphiphiles (Fig. 5c).[31] XRPD of xerogels from **5** and **6** in ethanol:water 1:1 mixture showed a similar broad pattern (Fig. S2d and e, ESI†).

Spectroscopic analysis

Considering the striking differences in the morphologies of the xerogels formed by glycosquaramides **5** and **6** (Fig. 4), we anticipated that the interactions between solvent and gelator molecules were critical in directing the SAFIN formation. In order to determine the nature of the driving forces of these self-assembly processes, we conducted some spectroscopic analyses. Preliminary ^{1}H-NMR studies of acetylated glycosquaramide **5** in (D_3)-acetonitrile were recorded (Fig. S3, ESI†). Upon increasing concentrations of **5**, only very small downfield shifts of the signals corresponding to the squaramide NH protons were observed ($\Delta \delta = 0.071$, 0.081 respectively), indicating weak intermolecular H-bonding. In this solvent, H-bonding interactions are less favoured than in other polar aprotic solvents.[32] One must also take into account that once the gelator molecules become assembled and form a rigid gel network, their signals are not visible in the ^{1}H-NMR spectra due to the long correlation times. The observed signals at higher concentrations would represent looser aggregates dissolved in the solvent entrapped

in the gel network.[33] Hence, we carried out FTIR studies to ascertain the role of H-bonding in gel formation.

Previous studies have shown that when organogel formation is promoted by H-bonding, the IR bands associated with the relevant functional groups in the molecule shift to lower wavenumbers compared to those recorded for the gelator free in solution.[34] FTIR spectra were recorded for glycosquaramides **5** and **6** in different physical states (*i.e.* as a bulk solid, in solution and throughout the gelation process). To study the gelation process, glycosyl squaramide **5** or **6** was dissolved in the corresponding solvent at CGC and heated above the gelation temperature. The solution was transferred into an IR solution transmission cell and spectra were recorded over a period of time (0–75 min), during which the cell cooled down to room temperature and gelation occurred. It was observed that the bands at the beginning of the experiment (time = 0, assigned to the solvated gelator molecules in solution) decreased in intensity and new bands associated with the formation of H-bonds appeared to concurrently grow (Fig. 6). At the end point of the experiment (time = 75 min), bands for compound **5** in both solution and gel

phase can be observed. This is consistent with the rheological data that indicated that gel formation can take up to 120 h to reach completion. Considering the increase in intensity of the bands for **5** in the gel phase as a function of time, it can be deduced that there is an induction period for gelation. This would indicate the existence of a free energy barrier to the nucleation process that is necessary for the gel phase to grow.

The positions and assignments of the noteworthy IR bands (stretching absorption bands for secondary amines, νNH, and carbonyl, νCO) of **5** and **6** in the three states are given in Table 4. All the NH stretch bands were observed between 3128 and 3385 cm^{-1}, indicating that squaramidic NHs are H-bonded. All samples also showed a small broad band at 1799 cm^{-1} corresponding to the ring breathing of the squaramide unit.[30] For gelator **5** in ethyl acetate, the νNH and νCO bands shifted to higher frequencies (105 and 28 cm^{-1}, respectively) between the solution and gel state, supporting the formation of H-bonds during the gelation process (Fig. 6a). The wavenumbers for the νNH and νCO bands in the solid and gel state are very similar, which could indicate inherent H-bonding in
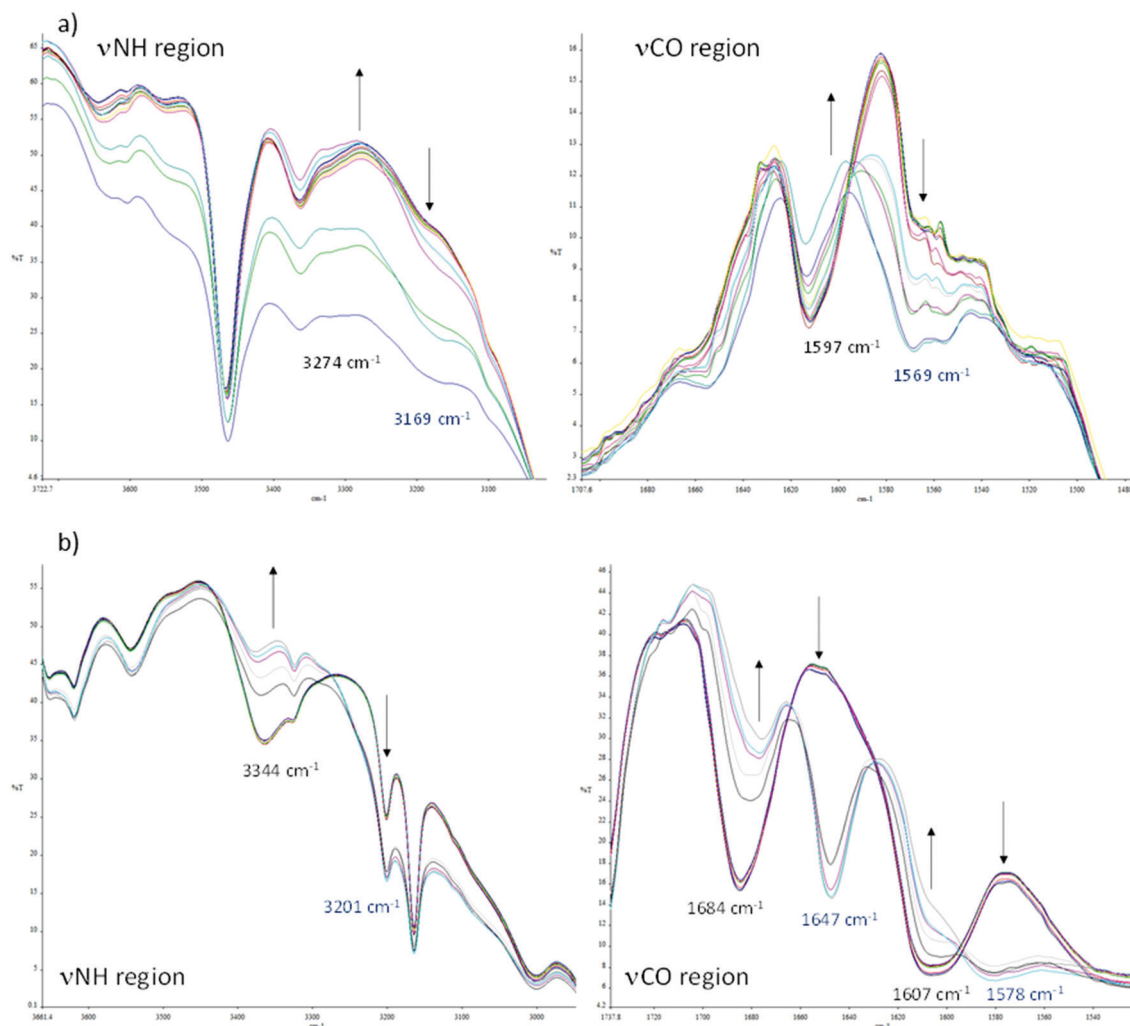

Fig. 6 FTIR spectra of compound **5** in (a) EtOAc (1.4% w/v) and (b) MeCN (0.9% w/v) from 0–75 min. The solution injected into the cell was warm and was allowed to cool to rt. Left – νNH region; right – νCO region.

Table 4 Position of characteristic IR bands of **5** and **6** in the solid state (NaCl plate or KBr disk), solution and gel state

Compound	Solvent	State	νNH (cm^{-1})	νCO (cm^{-1})	
5	—	Bulk (NaCl plate)	3174	1570	
	EtOAc	Solution	3274	1597	
		Gel	3169	1569	
	MeCN	Solution	3344	1684	1607
		Gel	3201	1647	1578
6	—	Bulk (KBr disk)	3233	1570	
	EtOH : H$_2$O (1 : 1)	Solution	Overlapping with solvent peaks	1569	
		Gel		1568	

the bulk material.[10] Interestingly, for gelator **5** in acetonitrile two distinct νCO bands can be appreciated, which suggests that more than one assembly mode can take place during the gelation process. The νNH and νCO bands shifted to higher frequencies (by 143, 37 and 29 cm^{-1}, respectively) between the solution and gel state, which again correlates well with H-bonding interactions (Fig. 6b). The wavenumbers for the νNH and νCO bands of compound **5** in the acetonitrile gel are slightly higher than in the ethyl acetate gel, which suggests weaker H-bonding interactions take place in acetonitrile.

The gelation processes of glycosyl squaramides in ethanol : water proved more difficult to investigate by FTIR; the νNH band of deprotected glycosyl squaramide **6** in solution and gel state in ethanol : water 1 : 1 mixture could not be distinguished from the overlapping solvent bands (Fig. S4, ESI†). No changes in the wavenumber corresponding to the absorption band of νCO in gelator **6** were observed between the bulk solid, solution or gel state (Table 4). When spectra were recorded using FTIR-ATR optics over a period of 1 h, the most appreciable change was the growth in intensity with time of the νCO band at 1569 cm^{-1} (Fig. S4, ESI†). This difference in intensity of the FTIR bands between the solution and gel state has been observed by other authors and is proposed to be due to an increase in the concentration of glycosyl squaramide **6** close to the ATR crystal as the gel forms.[35,36] Given the amphiphilic nature of this compound, aromatic interactions between squaramide rings[30] and hydrophobic interactions are expected to be the main driving force for gelation in the presence of water.

Conclusion

In summary, we report the first example of glycosyl squar-amides as supramolecular gelators. Compounds **2**, **3**, **5**, and **6** were prepared in three steps from accessible carbohydrate building blocks, using robust methodologies that proceeded in good yields. Evaluation of the gelation abilities of these compounds highlighted the importance of the aliphatic hydro-carbon chain: amphiphilic glycosyl squaramides **5** and **6** were found to effectively induce the formation of thermoreversible gels in polar aprotic organic solvents, ethanol and 1 : 1 mixtures of ethanol water at very low CGC. The rheological analysis showed the gels reach structural stability 120 h after formulation and have a high elastic character, leading to a higher structural integrity. Rheological characteristics of gels showed a clear dependence of gelator concentration. SEM imaging revealed very

different xerogel structures depending on the solvent, which indicates that solvent–gelator interactions dictate the SAFIN formation leading to distinct self-assembled structures. Spectro-scopic analysis reveals that H-bonding takes place in organogel formation, although intermolecular interactions of hydrophobic nature appear to be the major driving force for the gelation process. The synthetic versatility of the glycosyl squaramides described herein, together with their excellent gelation abilities and rheological properties showcases the potential of this new class of supramolecular materials in a range of applications currently being explored in our laboratory.

Conflicts of interest

There are no conflicts to declare.

Acknowledgements

References

1 P. R. A. Chivers and D. K. Smith, *Nat. Rev. Mater.*, 2019, **4**, 463.
2 J. W. Steed, *Chem. Commun.*, 2011, **47**, 1379.
3 S. Datta and S. Bhattacharya, *Chem. Soc. Rev.*, 2015, **44**, 5596.
4 N. Basu, A. Chakraborty and R. Ghosh, *Gels*, 2018, **4**, 52.
5 R. I. Storer, C. Aciro and L. H. Jones, *Chem. Soc. Rev.*, 2011, **40**, 2330.
6 L. A. Marchetti, L. K. Kumawat, N. Mao, J. C. Stephens and R. B. P. Elmes, *Chem*, 2019, **5**, 1398.
7 P. Chauhan, S. Mahajan, U. Kaya, D. Hack and D. Enders, *Adv. Synth. Catal.*, 2015, **357**, 253.
8 Y. Ohsedo, M. Miyamoto, A. Tanaka and H. Watanabe, *New J. Chem.*, 2013, **37**, 2874.
9 J. V. Alegre-Requena, M. Häring, I. G. Sonsona, A. Abramov, E. Marqués-López, R. P. Herrera and D. Díaz Díaz, *Beilstein J. Org. Chem.*, 2018, **14**, 2065.
10 J. Schiller, J. V. Alegre-Requena, E. Marqués-López, R. P. Herrera, J. Casanovas, C. Alemán and D. Díaz-Díaz, *Soft Matter*, 2016, **12**, 4361.

11 C. Tong, T. Liu, V. Saez-Talens, W. E. M. Noteborn, T. H. Sharp, M. M. R. M. Hendrix, I. K. Voets, C. L. Mummery, V. V. Orlova and R. E. Kieltyka, *Biomacromolecules*, 2018, **19**, 1091.

12 C. López, M. Ximenis, F. Orvay, C. Rotger and A. Costa, *Chem. – Eur. J.*, 2017, **23**, 7590.

13 S. Bujosa, E. Castellanos, A. Frontera, C. Rotger, A. Costa and B. Soberats, *Org. Biomol. Chem.*, 2020, **18**, 888.

14 A. Brito, Y. M. Abul-Haija, D. Soares da Costa, R. Novoa-Carballal, R. L. Reis, R. V. Ulijn, R. A. Pires and I. Pashkuleva, *Chem. Sci.*, 2019, **10**, 2385.

15 J. Qi, Y. Yan, B. Cheng, L. Deng, Z. Shao, Z. Sun and X. Li, *ACS Appl. Mater. Interfaces*, 2018, **10**, 6180.

16 C. Rizzo, J. L. Andrews, J. W. Steed and F. D'Anna, *J. Colloid Interface Sci.*, 2019, **548**, 184.

17 B. O. Okesola and D. K. Smith, *Chem. Soc. Rev.*, 2016, **45**, 4226.

18 A. Varki, *Glycobiology*, 2016, **27**, 3.

19 F. D. Tropper, F. O. Andersson, S. Braun and R. Roy, *Synthesis*, 1992, 618.

20 Z. Bobcheva, D. Zhiryakova and M. Guncheva, *J. Enzyme Inhib. Med. Chem.*, 2011, **26**, 587.

21 S. Orlandi, R. Annunziata, M. Benaglia, F. Cozzi and L. Manzoni, *Tetrahedron*, 2005, **61**, 10048.

22 S. Kiyonaka, S. Shinkai and I. Hamachi, *Chem. – Eur. J.*, 2003, **9**, 976.

23 X. Zhang, S. Lee, Y. Liu, M. Lee, J. Yin, J. L. Sessler and J. Yoon, *Sci. Rep.*, 2014, **4**, 4593.

24 H. Chen, F. Xie, L. Chen and B. Zheng, *J. Food Eng.*, 2019, **244**, 150.

25 N. Zanna and C. Tomasini, *Gels*, 2017, **3**, 39.

26 M. Cassanelli, I. Norton and T. Mills, *Food Struct.*, 2017, **14**, 112.

27 J. M. Poolman, J. Boekhoven, A. Besselink, A. G. Olive, J. H. van Esch and R. Eelkema, *Nat. Protoc.*, 2014, **9**, 977.

28 M. J. Kamlet, J. L. M. Abboud, M. H. Abraham and R. W. Taft, *J. Org. Chem.*, 1983, **48**, 2877.

29 E. A. Smith and P. K. Dea, *Applications of Calorimetry in a Wide Context - Differential Scanning Calorimetry, Isothermal Titration Calorimetry and Microcalorimetry*, InTech, 2013, pp. 407–444, , DOI: 10.5772/51882.

30 V. Saez-Talens, P. Englebienne, T. T. Trinh, W. E. M. Noteborn, I. K. Voets and R. E. Kieltyka, *Angew. Chem., Int. Ed.*, 2015, **54**, 10502.

31 Y. Huang and S. Gui, *RSC Adv.*, 2018, **8**, 6978.

32 L. Martínez, A. Sampedro, E. Sanna, A. Costa and C. Rotger, *Org. Biomol. Chem.*, 2012, **10**, 1914.

33 B. Escuder, M. LLusar and J. F. Miravet, *J. Org. Chem.*, 2006, **71**, 7747.

34 M. Suzuki, M. Yumoto, H. Shirai and K. Hanabusa, *Chem. – Eur. J.*, 2008, **14**, 2133.

35 J. Ramos, S. Arufe, R. O'Flaherty, D. Rooney, R. Moreira and T. Velasco-Torrijos, *RSC Adv.*, 2016, **6**, 108093.

36 F. X. Simon, T. T. T. Nguyen, N. Díaz, M. Schmutz, B. Demé, J. Jestin, J. Combet and P. J. Mésini, *Soft Matter*, 2013, **9**, 8483.